Audio Engineering Society

Convention Paper

Presented at the 126th Convention
2009 May 7–10 Munich, Germany

Alterations of the Temporal Spectrum in High-Resolution Sound Field Reproduction of Different Spatial Bandwidths

Jens Ahrens and Sascha Spors

Deutsche Telekom Laboratories, Technische Universität Berlin, Ernst-Reuter-Platz 7, 10587 Berlin, Germany

Correspondence should be addressed to Jens Ahrens (`jens.ahrens@telekom.de`)

ABSTRACT

We present simulations of the wave field reproduced by a discrete circular distribution of loudspeakers. The loudspeaker distribution is driven either with signals of infinite spatial bandwidth (as it happens in wave field synthesis), or the loudspeaker distribution is driven with signals of finite spatial bandwidth (as it is the case in near-field compensated higher order Ambisonics). The different spatial bandwidths lead to different properties both of the desired component of the reproduced wave field as well as of the spatial discretization artifacts. Our investigation focuses on the potential consequences of the artifacts on human perception.

1. INTRODUCTION

Since a few decades, the technical and theoretical means to use array technology in order to physically recreate sound fields have become widely available. These approaches are typically referred to as massive multichannel techniques. The most frequently implemented ones are near-field compensated higher Order Ambisonics (HOA), e.g. [1, 2] and wave field synthesis (WFS), e.g. [3, 4].

It has been recently shown by the authors [5] that the spatial bandwidth of the secondary source (i.e. loudspeaker) driving signal has fundamental influence on the properties of the reproduced wave field when spatially discrete secondary source distributions (i.e. loudspeaker setups) are considered. More explicitly, the spatial bandwidth of the driving function has a fundamental influence on the properties of the desired component of the reproduced wave field[1] as well as on the structure and energy distri-

[1]In this context, the term *desired component* refers to that component of the reproduced wave field which is desired to be reproduced. These components are opposed to spatial discretization artifacts which are superposed undesired artifacts.

bution of spatial discretization artifacts. However, analyses of the consequences on human perception are only partly available, e.g. in [6].
Note that we exclusively consider the physical reconstruction/reproduction of sound fields in this paper. At this stage, we do not take into account any psychoacoustic optimizations such as performed in [7, 8].
In this paper, we make frequent use of the following abbreviations:

- FSB: finite spatial bandwidth
- ISB: infinite spatial bandwidth
- SSD: secondary source distribution

2. THEORY

We briefly revisit the theory of sound field reproduction relevant to the presented investigations in this section. Refer to [5, 2, 4] for an extensive treatment.
The sample scenario under consideration in this paper is a virtual plane wave reproduced by a circular distribution of secondary line sources (i.e. purely 2D reproduction). The choice of a plane wave is justified since arbitrary propagating wave fields can be described by an appropriate superposition of plane waves.
The secondary line sources are positioned perpendicular to the target plane (the receiver plane). For convenience we specialize the formulation to this particular case. Our approach is therefore not directly implementable since loudspeakers exhibiting the properties of line sources are commonly not available. Real-world implementations usually employ loudspeakers with closed cabinets as secondary sources. The properties of these loudspeakers are more accurately modeled by point sources.
The main motivation to focus on two dimensions is to keep the mathematical formulation simple in order to illustrate the fundamental properties. The extension both to three-dimensional reproduction (i.e. spherical arrays of secondary point sources) and to two-dimensional reproduction employing circular arrangements of secondary point sources (*2½-dimensional reproduction*) is straightforward and a general treatment thereof can be found e.g. in [2, 4].
In the present paper, we compare FSB reproduction to ISB reproduction. As will be shown below, for both types of reproduction either of the established sound field reproduction methods (i.e. HOA and WFS) can be employed resulting in very similar properties. However, HOA is typically used for FSB reproduction, WFS is typically used for ISB reproduction. We also follow this practice for convenience. We therefore review both formulations (HOA and WFS) in the following sections.

2.1. The Ambisonics-like approach

In this section, we briefly review the approach which is typically associated with near-field compensated higher order Ambisonics. In the remainder of this paper, we call this approach *Ambisonics-like* and not *Ambisonics* since the term Ambisonics (and also near-field compensated higher order Ambisonics) refers to a specific approach which has evolved over many years and whose nomenclature is not perfectly compatible to the presented approach (compare e.g. to [1]). The formulation treated in this section has been presented by the authors in [2, 5]. Its physical fundament is the so-called *simple source approach*. The simple source approach for interior problems states that the acoustic field generated by events outside a volume can also be generated by a continuous distribution of secondary simple sources enclosing the respective volume [9].
The reproduction equation for a continuous circular distribution of secondary line sources and with radius r_0 centered around the origin of the coordinate system is then given by [5]

$$P(\mathbf{x},\omega) = \int_0^{2\pi} D(\alpha_0,\omega)\; G_{\mathrm{2D}}(\mathbf{x}-\mathbf{x}_0,\omega)\; r_0 \; d\alpha_0 \;, \quad (1)$$

where $\mathbf{x}_0 = r_0 \cdot [\cos\alpha_0 \;\; \sin\alpha_0]^T$. $P(\mathbf{x},\omega)$ denotes the reproduced wave field, $D(\alpha_0,\omega)$ the driving function for the secondary source situated at $\mathbf{x}_0$, and $G_{\mathrm{2D}}(\mathbf{x}-\mathbf{x}_0,\omega)$ its two-dimensional spatio-temporal transfer function.
A fundamental property of (1) is its inherent non-uniqueness and ill-posedness [10]. I.e. in certain situations, the solution is undefined and so-called *critical* or *forbidden frequencies* arise. The forbidden frequencies represent the resonances of the cavity under consideration. However, there are indications that the forbidden frequencies are only of minor relevance when practical implementations are consid-

ered [9].
Equation (1) constitutes a circular convolution and therefore the convolution theorem

$$\mathring{P}_\nu(r,\omega) = 2\pi r_0 \; \mathring{D}_\nu(\omega) \; \mathring{G}_\nu(r,\omega) \tag{2}$$

applies [11]. $\mathring{P}_\nu(r,\omega)$, $\mathring{D}_\nu(\omega)$, and $\mathring{G}_\nu(r,\omega)$ denote the Fourier series expansion coefficients of $P(\mathbf{x},\omega)$, $D(\alpha,\omega)$, and $G_{2\mathrm{D}}\left(\mathbf{x} - [r_0 \; 0]^T\right)^2$.
Equation (2) can be solved for $\mathring{D}_\nu(\omega)$. The secondary source driving function $D(\alpha_0,\omega)$ for a secondary source situated at position $\mathbf{x}_0$ reproducing a desired wave field with expansion coefficients $\breve{P}_\nu(\omega)$ can then be determined as [5]

$$D(\alpha,\omega) = \frac{1}{2\pi r_0} \sum_{\nu=-\infty}^{\infty} \frac{\breve{P}_\nu(\omega)}{\breve{G}_\nu(\omega)} e^{j\nu\alpha} \; , \tag{3}$$

whereby we omitted the index 0 in α_0 for convenience. Note that $D(\alpha,\omega)$ is independent from the receiver position. The coefficients $\breve{F}_\nu(\omega)$ of a function $F(\mathbf{x},\omega)$ are defined via

$$F(\mathbf{x},\omega) = \sum_{\nu=-\infty}^{\infty} \underbrace{\breve{F}_\nu(\omega) J_\nu\left(\frac{\omega}{c} r\right)}_{\mathring{F}_\nu(\omega,r)} e^{j\nu\alpha} \; , \tag{4}$$

whereby $J_\nu(\cdot)$ denotes the ν-th order Bessel function [9]. Refer to [5] for the explicit driving function for the considered scenario of a virtual plane wave reproduced by a circular distribution of secondary line sources.
The driving function (3) is not per se spatially bandlimited (ν can take any integer value). However, (3) straightforwardly allows to apply a spatial bandlimitation (refer also to section 2.3). In the latter case, the summation over ν is only performed between the limits $-N$ and N. One then speaks of a spatial bandwidth of N respectively of N-th order reproduction.

2.2. Wave field synthesis

Wave field synthesis (WFS) is derived from the Kirchhoff-Helmhotz integral [4]. The Kirchhoff-Helmhotz integral states that the wave field inside a given source-free volume is uniquely defined by the sound pressure and the pressure gradient on the boundary of the respective volume [9]. Reinterpreted for reproduction purposes, this means that any source-free wave field can be reproduced inside a given volume by a continuous layer of secondary monopole and dipole sources enclosing the volume. The employment of dipole sources is inconvenient since loudspeakers behaving like dipoles are commonly not available.
When some restrictions are accepted, the necessity of an enclosing SSD can be omitted. The SSD then has to have infinite extend. When the SSD is then also planar, the dipole sources can be replaced by simply doubling the strength of the remaining monopole sources. As stated above, this approach is only physically correct for planar continuous SSD with infinite extend.
However, curved SSD can be interpreted as being locally planar. If the SSD under consideration is also convex, then the above described monopole-only approach can be applied with only moderate error [5, 4]. Note that the driving signal which is applied assumes a particular spatio-temporal transfer function of the involved secondary sources which is dependent on the geometry of the SSD. The spatio-temporal transfer function of the actually employed secondary sources is typically assumed to be omnidirectional. This circumstance is referred to as Green's function mismatch and is the reason why WFS provides only approximate reproduction for non-planar SSDs.
The reproduction equation for WFS employing a continuous circular distribution of secondary line sources and centered around the origin of the coordinate system is given by [5]

$$P(\mathbf{x},\omega) = \int_0^{2\pi} \underbrace{-2a(\alpha_0)\frac{\partial}{\partial \mathbf{n}} S(\mathbf{x},\omega)\big|_{\mathbf{x}=\mathbf{x}_0}}_{D(\alpha_0,\omega)} \times \\ \times G_{2\mathrm{D}}(\mathbf{x}-\mathbf{x}_0,\omega) \; r_0 \; d\alpha_0 \; , \tag{5}$$

Again $\mathbf{x}_0 = r_0 \cdot [\cos\alpha_0 \;\; \sin\alpha_0]^T$, $P(\mathbf{x},\omega)$ denotes the reproduced wave field, $S(\mathbf{x},\omega)$ the desired wave field, $D(\alpha_0,\omega)$ the driving function for the secondary source situated at $\mathbf{x}_0$, and $G_{2\mathrm{D}}(\mathbf{x}-\mathbf{x}_0,\omega)$ its two-dimensional spatio-temporal transfer function. The term $a(\alpha_0)$ denotes a window function which takes

[2] Note that the coefficients $\mathring{G}_\nu(r,\omega)$ as used throughout this paper assume that the secondary source is situated at the position ($r = r_0, \alpha = 0$) and is orientated towards the coordinate origin.

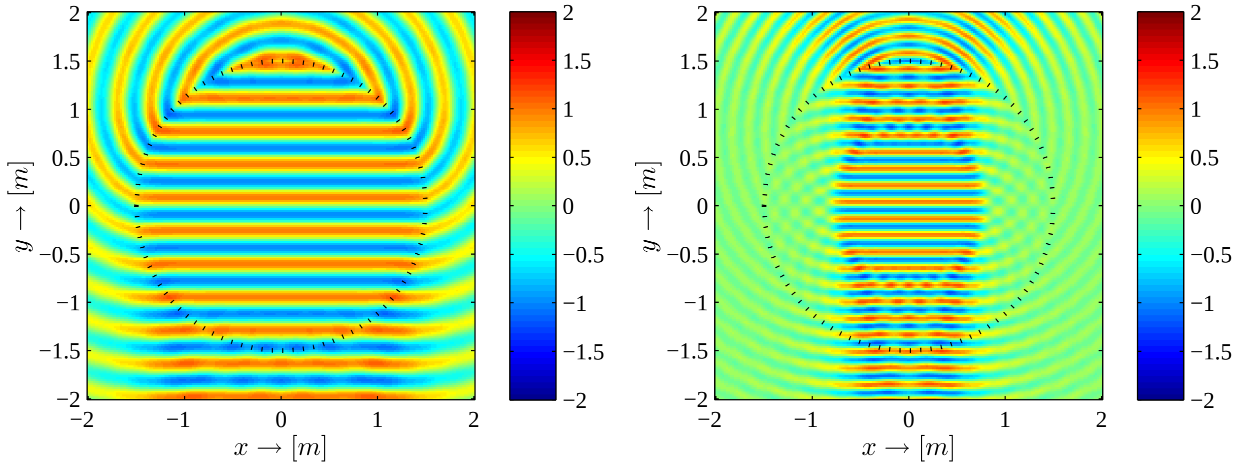

(a) $f = 1000$ Hz.

(b) $f = 2000$ Hz.

Fig. 1: $\Re\{P(\mathbf{x})\}$ of a continuous SSD reproducing a plane wave of different temporal frequencies. A spatial bandwidth limitation of $N = 27$ is applied.

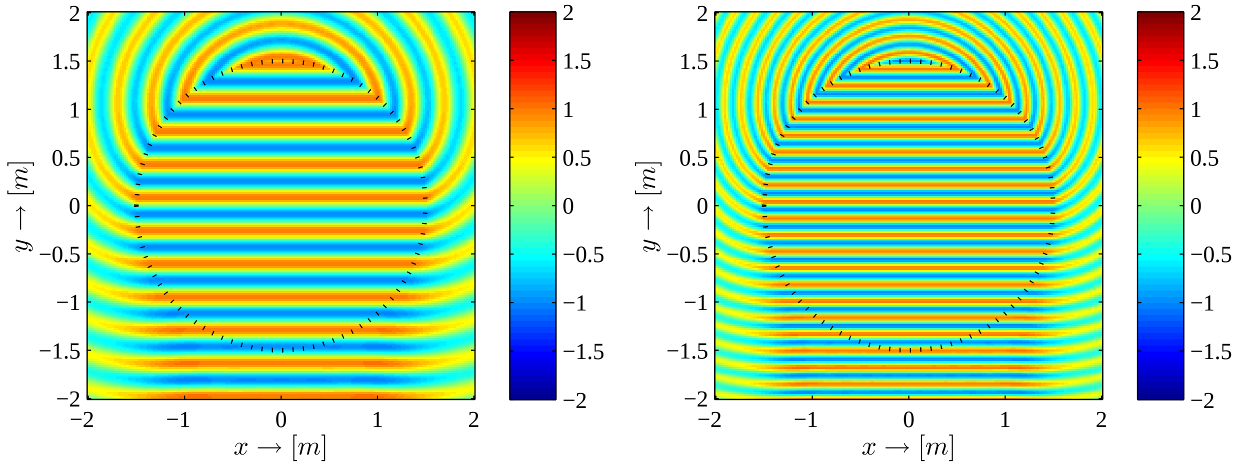

(a) $f = 1000$ Hz.

(b) $f = 2000$ Hz.

Fig. 2: $\Re\{P(\mathbf{x}, \omega)\}$ of a continuous SSD reproducing a plane wave of different temporal frequencies. No spatial bandwidth limitation applied ($N = \infty$).

care that only relevant secondary sources are driven (see below). Note the similarity of (1) and (5).
Equation (5) states that inside the SSD, the desired wave field $S(\mathbf{x}, \omega)$ is reproduced when the secondary sources are driven with the gradient of $S(\mathbf{x}, \omega)$ in direction of the inward pointing surface normal on the SSD evaluated at the position of the secondary source under consideration. Of course, outside the SSD the reproduced wave field does generally not correspond to the desired one. Although not appar-

ent from (5), in WFS employing a closed SSD like in the present paper, not all secondary sources do necessarily contribute to a given virtual (desired) wave field. Therefore, an appropriate selection has to be performed in order to identify unwanted contributions [12]. This selection is incorporated into the window function $a(\alpha_0)$ in (5). Refer to [5] for the explicit driving function for the considered scenario of a virtual plane wave reproduced by a circular distribution of secondary line sources.
Note that the secondary source driving function calculated according to (5) is generally not bandlimited with respect to the spatial bandwidth since typically chosen virtual wave fields $S(\mathbf{x}, \omega)$ such as plane or spherical waves are not bandlimited. This enables a very efficient implementation in the time domain [4]. Of course, also a spatially bandlimited wave field can be defined as desired wave field. This leads then to a similarly bandlimited driving function. However, the benefit of the efficient time domain driving function is given away and a summation similar to the one performed in the Ambisonics-like driving function (3) is necessary. The reproduced wave field is then approximately equal to the wave field reproduced by the same SSD driven with the according Ambisonics-like driving function of equal bandwidth. Due to the Green's function mismatch and the therewith necessary secondary source selection in WFS [5], minor errors arise which are assumed to be perceptually uncritical.

2.3. Spatial discretization

For the theoretic continuous secondary source distribution, any wave field which is source-free inside the secondary source distribution can be accurately reproduced apart from the forbidden frequencies in the Ambisonics-like approach (refer to section 2.1) respectively apart from a minor error due to the Green's function mismatch in WFS (refer to section 2.2). Real-world implementations of audio reproduction systems will always employ a finite number of discrete secondary sources. This spatial discretization constitutes spatial sampling and can result in spatial aliasing. In this section, we briefly review the consequences of spatial sampling. A thorough treatment can be found in [5, 2, 13].
It can be shown that the angular sampling of the driving function results in repetitions of the angular spectrum (i.e. in the present case the Fourier expansion coefficients $\mathring{D}_\nu(\omega)$) of the continuous driving function $D(\alpha, \omega)$ [13]

$$\mathring{D}_{\nu,S}(\omega) = \sum_{\eta=-\infty}^{\infty} \mathring{D}_{\nu+\eta L}(\omega) \ , \tag{6}$$

when L equiangular sampling points (i.e. loudspeakers) are taken. Equation (2) states that the angular spectrum of the reproduced wave field $\mathring{P}_\nu(r, \omega)$ is equal to the angular spectrum of the driving function $\mathring{D}_\nu(\omega)$ weighted by the angular spectrum of the secondary sources $\mathring{G}_\nu(r, \omega)$. Note that all angular spectra are taken with respect to the expansion around the origin of the global coordinate system.
In order to yield the angular spectrum $\mathring{P}_{\nu,S}(r, \omega)$ of the wave field reproduced by a discrete secondary source distribution, the spectral repetitions given by (6) have to be introduced into (2). The case of $\eta = 0$ then describes the desired component of the reproduced wave field. In other words: Despite sampling the desired component of the reproduced wave field is always present. Note that this in contrast to temporal aliasing [11]. The cases of $\eta \neq 0$ describe additional components due to sampling. These additional components can not be avoided.
As stated in sections 2.1 and 2.2, neither driving function (equations (3) and (5)) is per se bandlimited with respect to the angular frequency ν. Thus, when the angular bandwidth of the driving function is not artificially limited, the angular repetitions overlap and interfere.
In order to avoid such overlapping and interference of the spectral repetitions, the angular bandwidth of the continuous driving function of the Ambisonics-like approach (3) can be limited as

$$D_N(\alpha, \omega) = \frac{1}{2\pi r_0} \sum_{\nu=-N}^{N} \frac{\breve{P}_\nu(\omega)}{\breve{G}_\nu(\omega)} e^{j\nu\alpha} \ , \tag{7}$$

whereby $N = \frac{L-1}{2}$ when a discrete distribution of an odd number L of secondary sources is considered and accordingly for even L. Strictly spoken, when (7) is applied spatial aliasing is prevented in the driving function since no spectral overlaps occur. However, since the spatial spectrum $\mathring{G}_\nu(r, \omega)$ of the secondary sources is not bandlimited, spatial repetitions of the driving function will always be reproduced. Although this is rather a reconstruction

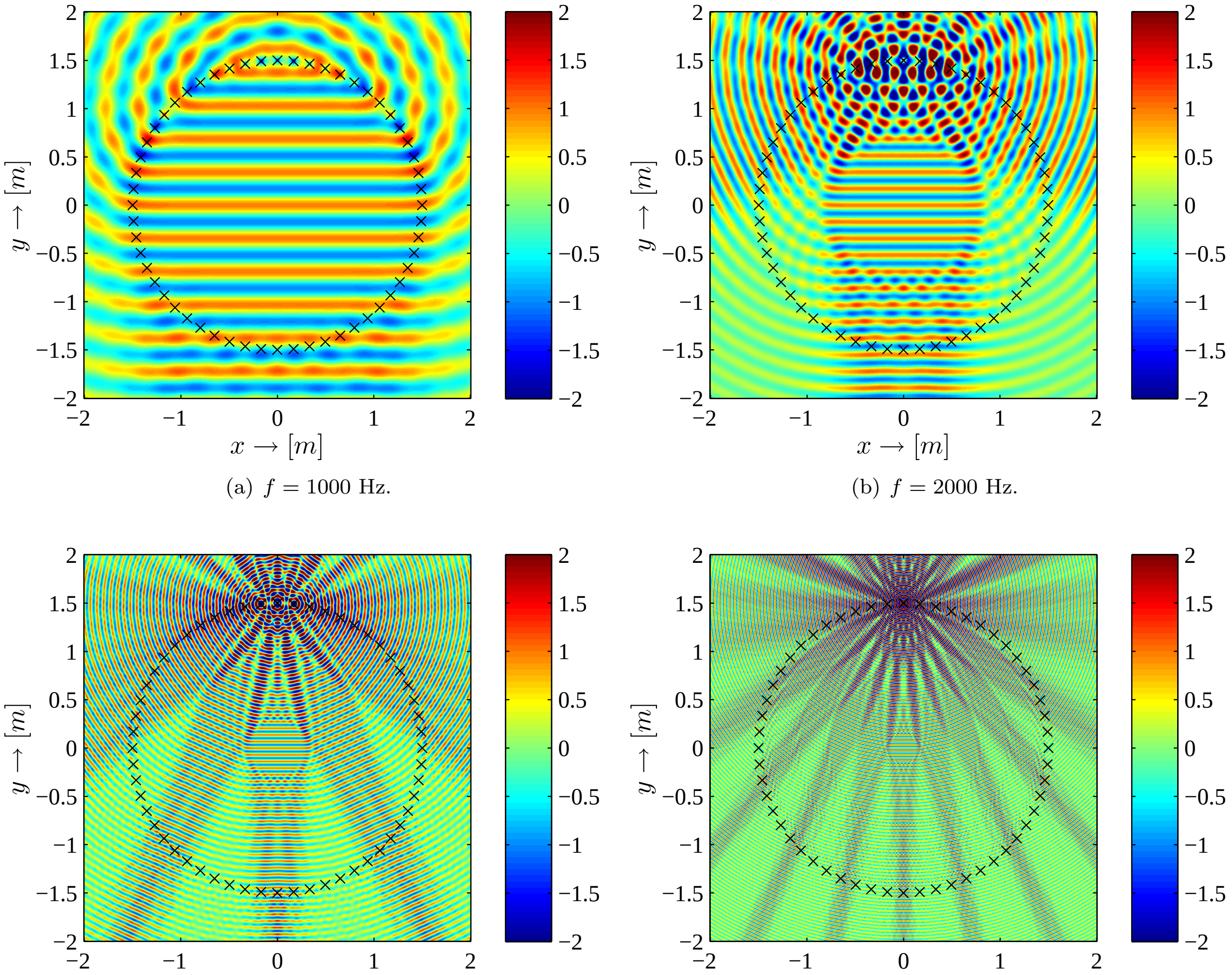

(a) $f = 1000$ Hz.

(b) $f = 2000$ Hz.

(c) $f = 5000$ Hz.

(d) $f = 10000$ Hz.

Fig. 3: $\Re\{P(\mathbf{x}, \omega)\}$ of a discrete SSD reproducing a plane wave of different temporal frequencies. A spatial bandwidth limitation of $N = 27$ is applied.

error [5] it is commonly also referred to as spatial aliasing. We do so as well in the remainder for convenience. Note that it is actually impossible to implement the Ambisonics-like approach (3) with infinite bandwidth since this would require an infinite summation.

A spatial bandlimitation like in (7) can not be straightforwardly applied in WFS (5). In order to achieve such a bandlimitation in WFS, a spatially bandlimited desired wave field based on the expansion (4) has to be formulated. The WFS driving function then exhibits the same spatial bandwidth like the desired wave field. However, we are not aware of an according implementation since as a matter of efficiency, WFS is typically implemented in the time domain [4].

As a consequence of the infinite spatial bandwidth, the repetitions in (6) always overlap in WFS and

spatial aliasing in the strict sense occurs.
When we speak of FSB reproduction in the remainder of this paper we refer to the Ambisonics-like driving function given by (7). When we speak of ISB reproduction in the remainder of this paper we refer to the WFS driving function indicated in (5).

3. CONTINUOUS SECONDARY SOURCE DISTRIBUTIONS

At a first stage, we consider the reproduction via continuous SSD. These provide reproduction which is perfectly free of spatial discretization artifacts. They therefore allow to independently investigate the properties of the desired component of the reproduced wave field. For convenience, we consider a virtual plane wave as desired wave field to be reproduced.
It can be shown that continuous SSD reproduce a wave field with exactly the same spatial bandwidth like the driving function [5, 2]. Therefore, continuous SSD driven with FSB reproduce a wave field of FSB, continuous SSD driven with ISB reproduce a wave field of ISB. This constitutes the first essential difference between the two reproduction approaches. Refer to figures 1 and 2 for an illustration of the general properties. The most important properties are summarized in the following list:

- For low frequencies, the reproduction is accurate both for FSB and ISB (refer to figures 1(a) and 2(a)).
- For higher frequencies, the energy of the reproduced wave field concentrates around the center of the secondary source distribution in FSB systems (refer to figure 1(b)). This is a direct consequence of the spatial bandwidth limitation and is reflected by the properties of the involved Bessel functions. This concentration of the energy around the center of the SSD is more pronounced the higher the temporal frequency. In other words, for receiver positions outside the center, high frequencies are significantly attenuated (by several dB). Therefore, timbral coloration might occur.
- In ISB systems, the reproduction is accurate for all temporal frequencies (refer to figure 2(b)) and no impairment is to be expected.

4. WAVE FIELDS REPRODUCED BY DISCRETE SECONDARY SOURCE DISTRIBUTIONS

In this section, we move further to discrete SSD. This is what we find in real-world implementations (refer also to section 2.3). Again, we consider a virtual plane wave as desired wave field to be reproduced.
Below a certain critical frequency which we term *spatial aliasing frequency* the ratio of the energy of spatial discretization artifacts and the energy of the desired component of the reproduced wave field is very low and the reproduction is considered aliasing-free. Above the spatial aliasing frequency, the above described energy ratio rises quickly and reproduction is considered being corrupted by spatial aliasing.
The artifacts which arise due to the spatial discretization are superposed to those artifacts due to spatial bandwidth limitation as described in section 3. The properties of the discretization artifacts are strongly related to the spatial bandwidth of the driving function (refer to section 2) and can therefore not be treated independently.

4.1. Finite spatial bandwidth reproduction

The general properties of discrete SSD driven with FSB signals can be deduced from figure 3 and are summarized in the following list:

- The center of the SSD stays essentially free of aliasing artifacts. The higher is the frequency, the smaller is this sweet area.
- Outside the sweet area, strong aliasing artifacts arise.
- The energy of the aliasing artifacts is not equally distributed over the receiver area. I.e., the energy of the artifacts is strongly dependent on the position. This indicates that also the perception is strongly dependent on the listener position.
- The spatial structure of the aliasing artifacts is quite regular. The latter can locally be interpreted as plane wave fronts originating from that point on the secondary source contour where the desired virtual plane wave arrives. This could result in a localization bias and

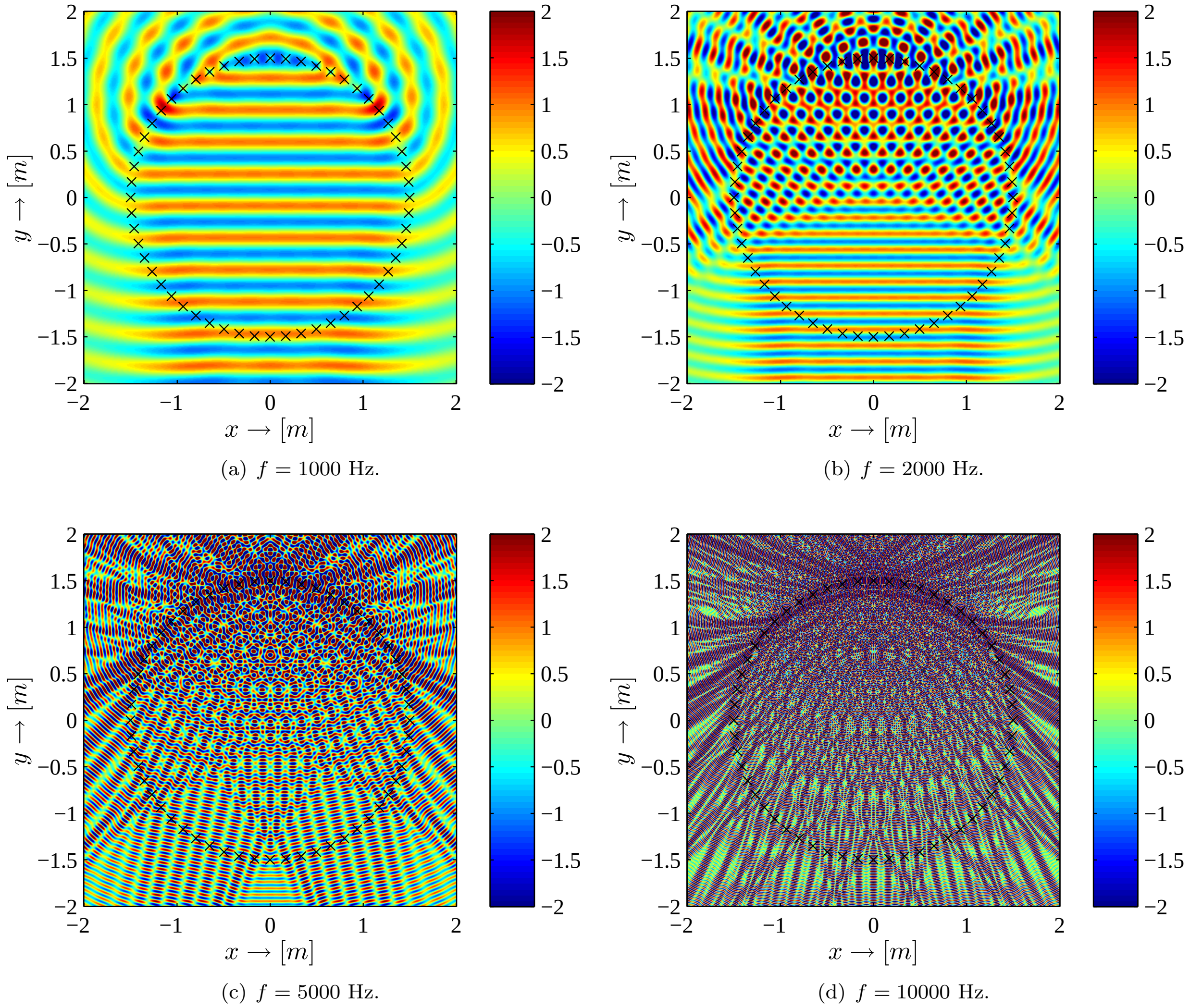

Fig. 4: $\Re\{P(\mathbf{x}, \omega)\}$ of a discrete SSD reproducing a plane wave of different temporal frequencies. No spatial bandwidth limitation applied ($N = \infty$).

impair the localization quality of the virtual source. Refer to section 6 for a further discussion.

4.2. Infinite spatial bandwidth reproduction

The general properties of discrete SSD driven with ISB signals can be deduced from figure 4 and are summarized in the following list:

- No prominent sweet spot or sweet area arises.
- The energy of the aliasing artifacts is distributed rather homogenously over the receiver area. No strong position dependent variation of the aliasing artifacts arises.
- The artifacts do not exhibit an obvious spatial structure. The preceptive impairment can be expected to be less critical than with FSB reproduction.

5. SPECTRA OF THE WAVE FIELDS REPRODUCED BY DISCRETE SECONDARY SOURCE DISTRIBUTIONS

In order to get more insight into the consequences of the different energy distributions in the receiver area, we present the transfer function of the discrete SSD under consideration when driven with varying spatial bandwidths for selected receiver positions. As in the previous sections, the desired wave field to be reproduced is a plane wave.

Figures 5(a), 5(b) and 6(a), 6(b) illustrate the global variation of the absolute value of the transfer function between the SSD and selected receiver positions, i.e. we investigate a selection of receiver points which are distributed over the entire receiver area.

Figures 5(c), 5(d) and 6(c), 6(d) illustrate the local variation of the absolute value of the transfer function, i.e. we investigate a selection of receiver points which are located within the vicinity of each other.

Observations for FSB reproduction:

- A sweet spot with perfectly flat frequency response is apparent in the center of the secondary source distribution (refer to the black line in figures 5(a) and 5(b)).
- Obvious variations of the absolute value of the transfer function arise above the aliasing frequency for positions along the x-axis (refer to figure 5(a)).
- For positions along the y-axis strong variations arise (refer to figure 5(b)).
- Only minor variation is apparent when moving around a selected position on the x-axis (refer to figure 5(c)). The general properties of the transfer function stay similar.
- The same holds true for the vicinity of a position on the y-axis (refer to figure 5(d)). In this case the deviation from the desired flat frequency response is significantly stronger than for lateral positions.
- Below the aliasing frequency (around 1.5 kHz), the transfer function is perfectly flat.

Observations for ISB reproduction:

- No sweet spot is apparent.
- For both global (figures 6(a) and 6(b)) and local (figures 6(c) and 6(d)) variations of the position, strong deviations from the desired flat response arise. In both cases the general properties of the transfer function are similar: (a) Many peaks and dips and (b) a high-pass character.
- Above the spatial aliasing frequency, spatial aliasing adds energy to the transfer function. The resulting high-pass character of the transfer function is very similar for all receiver positions and can therefore be compensated for via application of a prefilter. In real-world implementations of 2.5D WFS this is accomplished as follows: The 2.5D driving function for continuous SSD requires a prefilter with frequency response proportional to $\sqrt{j\frac{\omega}{c}}$ over the entire frequency range. This represents a high-pass with a constant slope of 3 dB per octave. Due to the fact that discrete SSDs have to be employed, spatial aliasing occurs and imposes a high-pass character onto the transfer function of the system *above* the spatial aliasing frequency. This high-pass character due to spatial aliasing substitutes the 3-dB-prefilter that the driving function dictates. The latter is therefore only applied below the spatial aliasing frequency.
- Even below the aliasing frequency, deviations from the desired flat frequency response arise. This is most likely a consequence of the Green's function mismatch which is apparent in WFS (refer to section 2.2). However, a detailed analysis is still to be performed.

It is reported in the literature [6] that the perceived timbral coloration in WFS (i.e. for ISB reproduction) is much less pronounced than would be expected from above simulations. When the receiver slightly changes his/her position, e.g. when a listener moves his/her head, he/she is exposed to transfer functions with very different behavior (figure 6). This is already the case even for very small movements. It is assumed that some kind of averaging

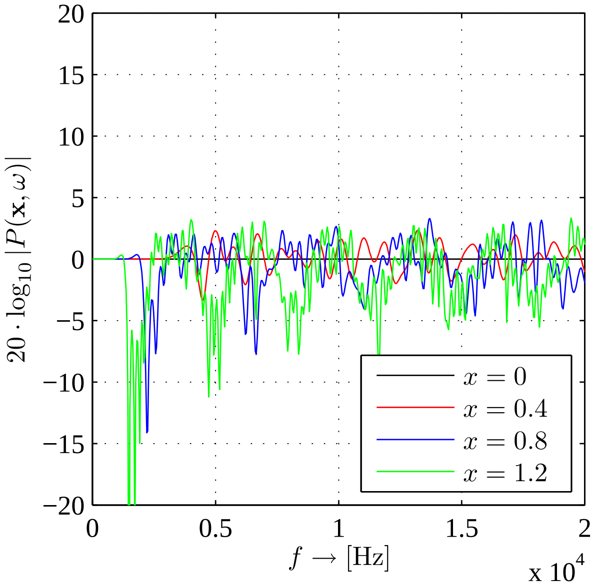

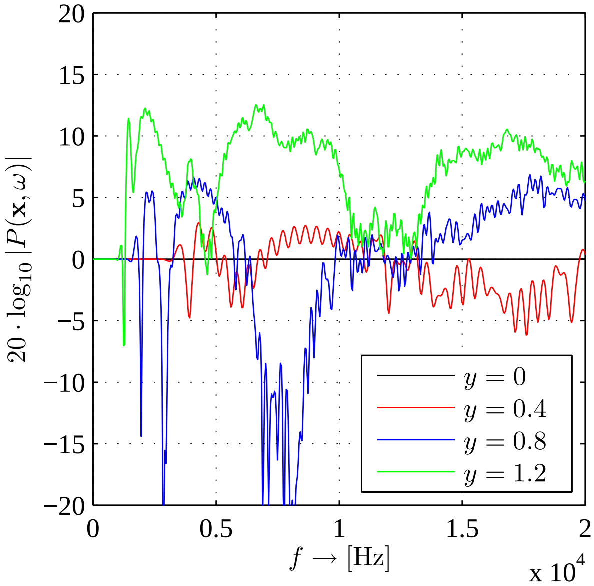

(a) Global variation. Positions from $\mathbf{x} = [0\ 0]^T$ to $\mathbf{x} = [1.2\ 0]^T$ in steps of 40 cm.

(b) Global variation. Positions from $\mathbf{x} = [0\ 0]^T$ to $\mathbf{x} = [0\ 1.2]^T$ in steps of 40 cm.

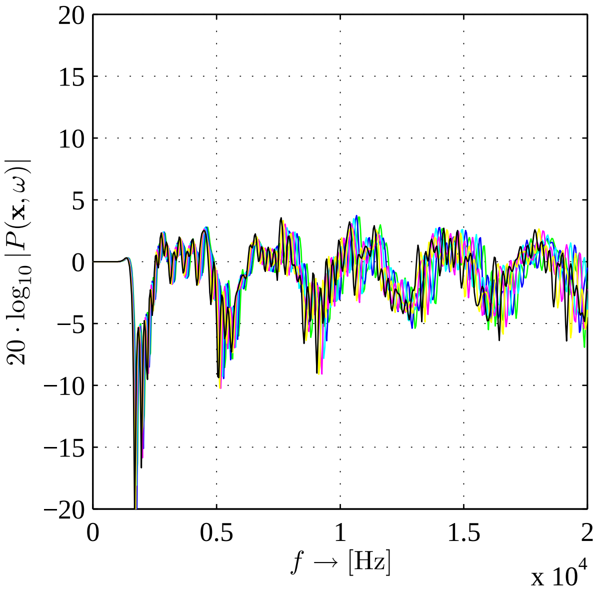

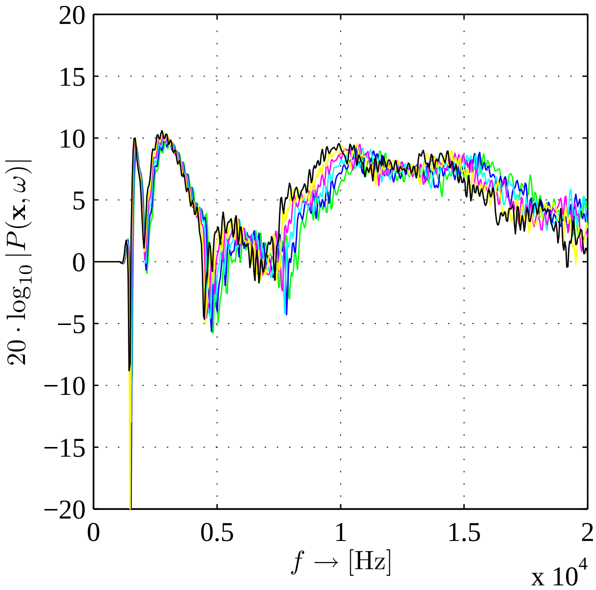

(c) Local variation. Positions from $\mathbf{x} = [1\ 0]^T$ to $\mathbf{x} = [1.05\ 0]^T$ in steps of 1 cm.

(d) Local variation. Positions from $\mathbf{x} = [0\ 1]^T$ to $\mathbf{x} = [1\ 1.05]^T$ in steps of 1 cm.

Fig. 5: Variations of the absolute value of the temporal transfer function of a discrete SSD to selected receiver positions. Spatial bandwidth limitation applied ($N = 27$).

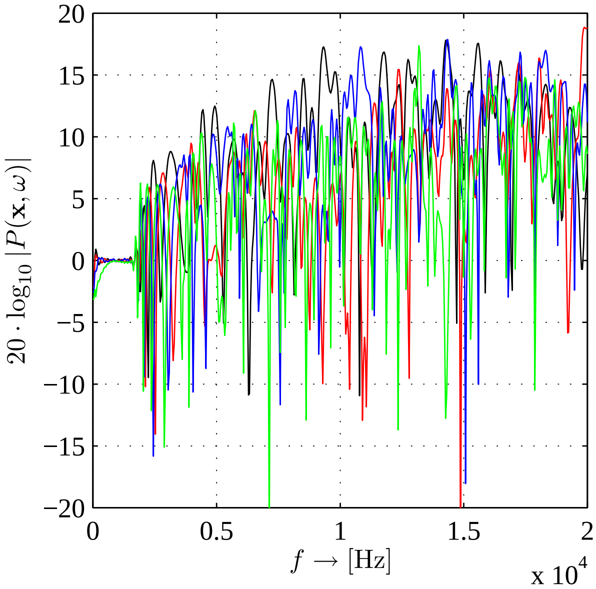

(a) Global variation. Positions from $\mathbf{x} = [0\ 0]^T$ to $\mathbf{x} = [1.2\ 0]^T$ in steps of 40 cm.

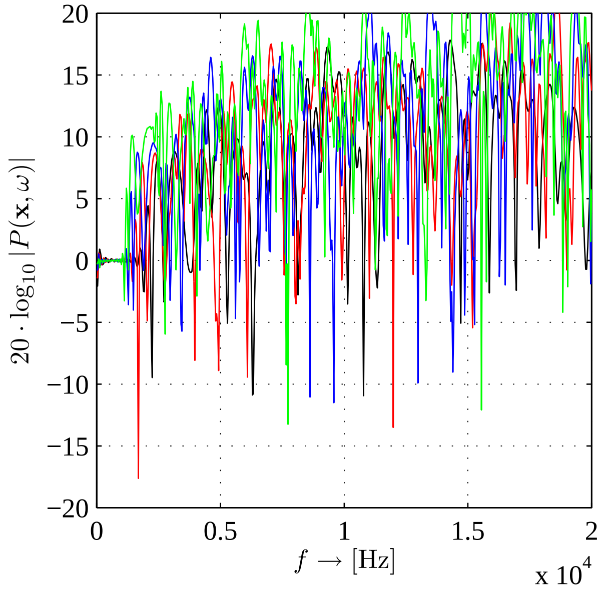

(b) Global variation. Positions from $\mathbf{x} = [0\ 0]^T$ to $\mathbf{x} = [0\ 1.2]^T$ in steps of 40 cm.

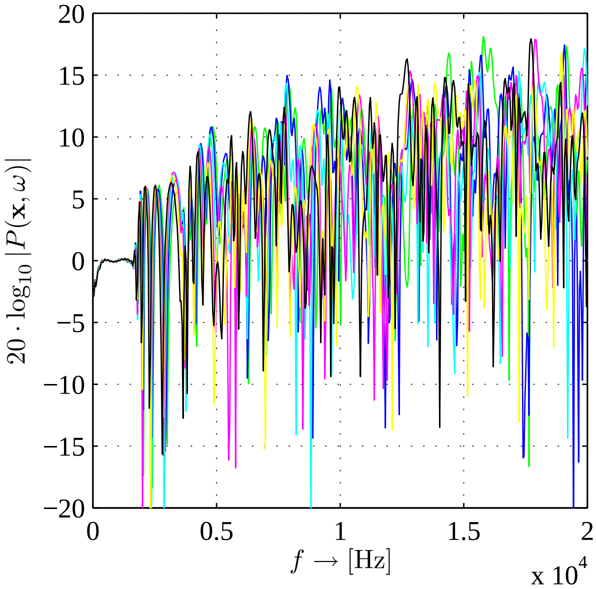

(c) Local variation. Positions from $\mathbf{x} = [1\ 0]^T$ to $\mathbf{x} = [1.05\ 0]^T$ in steps of 1 cm.

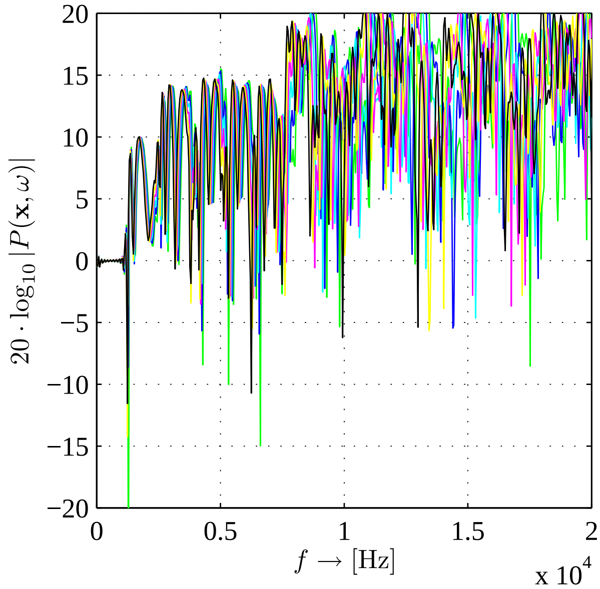

(d) Local variation. Positions from $\mathbf{x} = [0\ 1]^T$ to $\mathbf{x} = [1\ 1.05]^T$ in steps of 1 cm.

Fig. 6: Variations of the absolute value of the temporal transfer function of a discrete SSD to selected receiver positions. No bandwidth limitation applied ($N = \infty$).

takes place in the human auditory system which significantly levels out local variations in the transfer function.
Revisiting figures 5(c) and 5(d), we see that the local variation in the temporal transfer function of FSB reproduction is much less pronounced. The general properties of the transfer function stay similar so that we do not expect perceptual averaging to the same extend like in ISB reproduction. Since the general properties of the transfer function deviate strongly from the desired flat response we do expect a perceivable timbral coloration.

6. LOCALIZATION

As can be seen from figures 3(c) and 3(d), the spatial aliasing artifacts have a regular spatial structure in FSB reproduction. Locally, the spatial aliasing artifacts can be interpreted as plane wave fronts originating from that point on the secondary source contour where the desired plane wave front first hits the secondary source contour. As a consequence, listeners positioned outside the sweet area (the latter being almost aliasing-free) might localize the high-frequency content above the spatial aliasing frequency at the above mentioned position on the secondary source contour. The low-frequency content below the spatial aliasing frequency is localized in the direction where the plane wave comes. Note that there is no smooth transition between the two perceived source locations. Informal listening suggests that it might also happen that two individual virtual sources are perceived. Refer also to section 7.

In ISB, the energy of both the desired component of the reproduced wave field as well as of the spatial aliasing artifacts is evenly distributed over the entire receiver area. No spatial structure of the aliasing artifacts can be identified at this stage. It can therefore be expected that the impact of the spatial aliasing artifacts on localization is not as pronounced as in the case of FSB reproduction [6].

7. AMBISONICS AMPLITUDE PANNING

Traditional amplitude panning Ambisonics, e.g. [14, 15], is a simple technique to reproduce the spatially bandlimited approximation of the wave field of point sources positioned on the contour of the SSD. It is very convenient in the sense that the resulting driving function is a simple real-valued weighting of the virtual source's input signal. In terms of computational complexity, this approach is cheaper by several orders of magnitude compared to the FSB approach presented in section 2.1.
Now compare figures 3(c) and 7, the latter depicting

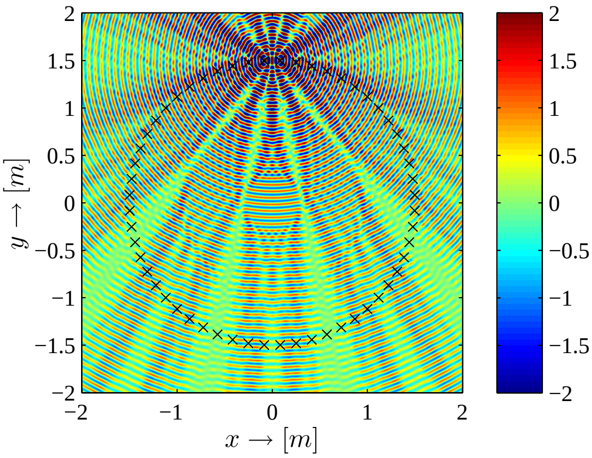

Fig. 7: $\Re\{P(\mathbf{x})\}$ of a discrete SSD driven by the traditional amplitude panning Ambisonics driving function for $f = 5000$ Hz. Compare to figure 3(c).

a simulation of amplitude panning Ambisonics. It can be seen that the reproduced wave fields looks very similar for such a high frequency which lies above the spatial aliasing frequency for most receiver locations. Note that in figure 7, the entire loudspeaker array was turned by $^{180}/_{56}$ degrees with respect to figure 3(c). This was done on order to avoid that the position of the resulting virtual point source coincides with one of the loudspeakers. Because in the latter case, the spatial aliasing artifacts are hardly distinguishable from the desired wave field and the resulting wave field looks almost free of aliasing artifacts.
In the FSB approach presented in section 2.1, the aliasing artifacts are only marginally affected by the relation between the positions of the secondary sources and the propagation direction of the desired plane wave. It might thus be that above the aliasing frequency, the FSB approach presented in section 2.1 provides more homogeneous reproduction of

arbitrary angles of incidence compared to Ambisonics amplitude panning by the cost of a significantly higher computational cost. However, the differences are subtle.
Of course, below the spatial aliasing frequency, the two approach can result in substantially different reproduced wave fields for certain receiver locations.
Note that above described findings are only valid for densely spaced SSD. Traditionally, Ambisonics amplitude panning is applied on SSD with low numbers of loudspeakers.

8. CONCLUSIONS

We have presented simulations of wave fields reproduced by a circular array of loudspeakers. We focused on an investigation of the artifacts arising in the reproduction of finite spatial bandwidth (FSB) compared to infinite spatial bandwidth (ISB). We chose an Ambisonics-like approach to represent FSB reproduction and wave field synthesis to represent ISB reproduction since this corresponds to common real-world implementations.
The major findings are: (1) in FSB reproduction, a pronounced sweet spot arises in the center of the secondary source distribution. This is not the case for ISB reproduction. (2) in ISB reproduction the energy of the spatial aliasing artifacts is rather evenly distributed over the receiver area. In FSB reproduction, the energy of spatial aliasing artifacts is heavily dependent on the position.
Our simulations suggest that the different properties of the aliasing artifacts for the two reproduction approaches are audible as timbral coloration and possibly also impairment of the localization quality of a virtual source. However, reliable conclusions can not be drawn from such simulations. A listening test to verify the results is in preparation.

9. REFERENCES

[1] J. Daniel. Représentation de champs acoustiques, application à la transmission et à la reproduction de scènes sonores complexes dans un contexte multimédia. PhD thesis Université Paris 6, 2001.

[2] J. Ahrens and S. Spors. An analytical approach to sound field reproduction using circular and spherical loudspeaker distributions. *Acta Acustica utd. with Acustica*, 94(6):988–999, Nov./Dec. 2008.

[3] A.J. Berkhout, D. de Vries, and P. Vogel. Acoustic control by wave field synthesis. *JASA*, 93(5):2764–2778, May 1993.

[4] S. Spors, R. Rabenstein, and J. Ahrens. The theory of wave field synthesis revisited. In *124th Convention of the AES*, Amsterdam, The Netherlands, May 17–20 2008.

[5] S. Spors and J. Ahrens. A comparison of wave field synthesis and higher-order Ambisonics with respect to physical properties and spatial sampling. In *125th Conv. of the AES*, San Francisco, CA, Oct. 2–5 2008.

[6] H. Wittek. Perceptual differences between wavefield synthesis and stereophony. PhD thesis, University of Surrey, 2007.

[7] M. A. Gerzon. Practical periphony: The reproduction of full-sphere sound. In *65th Convention of the AES*, London, UK, Feb. 25–28 1980.

[8] H. Wittek, F. Rumsey, and G. Theile. Perceptual enhancement of wavefield synthesis by stereophonic means. *JAES*, 2007.

[9] E. G. Williams. *Fourier Acoustics: Sound Radiation and Nearfield Acoustic Holography.* Academic Press, London, 1999.

[10] L. G. Copley. Fundamental results concerning integral representations in acoustic radiation. *JASA*, 44:28–32, 1968.

[11] B. Girod, R. Rabenstein, and A. Stenger. *Signals and Systems.* J.Wiley & Sons, 2001.

[12] S. Spors. Extension of an analytic secondary source selection criterion for wave field synthesis. In *123th Convention of the AES, New York, NY*, Oct. 2007.

[13] S. Spors and R. Rabenstein. Spatial aliasing artifacts produced by linear and circular loudspeaker arrays used for wave field synthesis. In *120th Convention of the AES, Paris, France*, May 20–23 2006.

[14] M.A. Gerzon. With-heigth sound reproduction. *JAES*, 21:2–10, 1973.

[15] M. Neukom. Ambisonic panning. In *123th Convention of the AES*, Oct. 5–8 2007.